Polym. Korea, Vol. 47, No. 5, pp. 613-627 (2023)
https://doi.org/10.7317/pk.2023.47.5.613

ISSN 0379-153X(Print)
ISSN 2234-8077(Online)

EPDM/NBR 나노복합체의 기계적 물성과 팽윤 저항에 대한 Nanosilica 영향 연구

S. Dhanasekar†, M.S. Ravi Theja*, S. Baskar**, and S. Vishvanathperumal

Department of Mechanical Engineering, S. A. Engineering College
*Department of Mechanical Engineering, Sri Eshwar College of Engineering, Coimbatore
**Centre for Nonlinear Systems, Chennai Institute of Technology, Kundrathur

(2023년 5월 5일 접수, 2023년 6월 26일 수정, 2023년 8월 8일 채택)

Effects of Nanosilica on the Mechanical Properties and Swelling Resistance of EPDM/NBR Nanocomposites

S. Dhanasekar†, M. S. Ravi Theja*, S. Baskar, and S. Vishvanathperumal**

Department of Mechanical Engineering, S.A. Engineering College, Chennai - 600077, Tamilnadu, India
**Department of Mechanical Engineering, Sri Eshwar College of Engineering, Coimbatore, Tamilnadu - 641202, Tamilnadu, India*
***Centre for Nonlinear Systems, Chennai Institute of Technology, Kundrathur, Chennai - 600069, Tamilnadu, India*

(Received May 5, 2023; Revised June 26, 2023; Accepted August 8, 2023)

Abstract: The final performance of polymer-based composites is greatly influenced by the surface modification of fillers, filler dispersion, and interfacial adhesion. In this contribution, silica is modified by polymethylhydrosiloxane (PMHS) using a quick and effective tris(pentafluorophenyl)borane-catalyzed functionalization that can be finished at room temperature in a few minutes. The modified silica exhibits both unaltered reactivity and a highly hydrophobic surface. A comparison of composites containing extracted silica and modified silica reveals that the PMHS modification can improve silica dispersibility by lowering the interfacial energy, as well as enhance interfacial interaction due to the reactivity of the remaining Si-H bonds. The modified composite shows remarkable improvements in mechanical properties with a PMHS grafting percentage as low as 1.5 wt% (63% increase in tensile strength, 12% increase in elongation at break, and 23% increase in modulus). We believe that the hydrosilane-modified silica offers enormous promise for the creation of high-performance polymer composites, owing to the improved overall performance of the modified composites and the ease and speed of the modification process.

Keywords: ethylene-propylene-diene monomer/acrylonitrile-butadiene rubber, extracted nanosilica, modified extracted nanosilica, nanocomposites.

Introduction

Blending techniques for making polymer compounds include latex, melt, and solution mixing.[1-3] Melt mixing is the most crucial process for creating polymer composites because the blend formed is pure, and the removal of water or solvent is not problematic. The solution mixing technique involves making a film from the chemicals produced after the polymer components are dissolved in an organic solvent.[4-5] Before being blended with a mixer in a rubber mixer, the components are heated for the latex mixing.[6-8] Rubber is a vital material frequently used in aerospace, automotive, marine, and medicinal applications due to its distinct characteristics. To achieve outstanding mechanical properties in rubber for specific applications, it must be chemically cross-linked and strengthened with fillers.[9-10] For this investigation, ethylene-propylene-diene monomer (EPDM) and acrylonitrile-butadiene rubber (NBR) were chosen due to their unique physical characteristics and incompatibility. EPDM is made of non-polar rubber, saturated (M-Class rubber), and has a very low -C=C- percentage. NBR, on the other hand, has more polar CN groups than other materials, increasing the cohesive energy density between the chains.

†To whom correspondence should be addressed.
gurusekar1989@gmail.com, ORCID 0000-0002-8766-8446

These categories are not present in EPDM. It is vital to remember that sulfur might potentially cause vulcanization of both EPDM and NBR during the co-crosslinking procedure, allowing crosslinking between the EPDM and NBR rubber.

Due to the lengthy and expensive complex processes, there are still a number of problems. Previously, a simple and affordable method of creating polymer composites was investigated, using conventional fillers like silica, nanoclays, and carbon blacks with the right coupling or compatibilizing agents.[11-13] This method improved filler dispersions and encouraged positive filler-matrix interactions. One of these processing aids commonly used to create these vulcanizates is Maleic anhydride (MAH) coupling or compatibilizing agent. Maleic acid is dehydrated to produce the chemical molecule known as MAH ($C_2H_2(CO)_2O$).[11-13] Kueseng *et al*.[11] previously employed a compatibilizer called MAH to successfully increase the interfacial adhesion of hydrophilic flax fibers to hydrophobic polymeric matrices. Additionally, Chow *et al.*[12] observed a notable improvement in the mechanical properties of Polyamide/Polypropylene (PA6/PP)-organoclay composites when they added EPDM-g-MAH compatibilizer to the mixture. In recent research by Azizli *et al*.,[14] the compatibilizer effects of EPDM-g-MAH and epoxidated natural rubber (ENR)-50 were investigated in carboxylated NBR (XNBR)/EPDM blends containing various types of nanoparticles (silica, carbon blacks, and Cloisites clays). The composites displayed improved physico-mechanical properties compared to those lacking compatibilizer or nanoparticles.

One of the most important food crops in the world is rice. One-fifth of the yearly gross rice production, known as rice husk, is wasted during the processing of the rice grains and is typically burned outdoors, which pollutes the environment and hinders progress. However, rice husk can be utilized to synthesize exceptionally pure silicon (Si), magnesium silicide (Mg_2Si), silicon carbide (SiC), silicon nitride (Si_3N_4), and other compounds for various purposes.[15]

Polymer nanocomposites, composed of nanoscale fillers and polymer matrices, have attracted significant attention in the past few decades.[16] Nanoparticles such as silica (SiO_2), carbon nanotubes (CNTs), clay (Cloisite-10A, -15A, -20A, -25A, -93A, and -30B), graphene, and others have been extensively used.[17]

Unfortunately, silica has a high degree of polarity due to the presence of silanol groups on its surface, leading to inadequate dispersion conditions in diene-based (non-polar) elastomers and poor contact between silica nanoparticles and the elastomer matrix. Considerable research and development have been dedicated to silica nanoparticles in rubber composites. Surface treatments, such as passivation by plasma or electron beam[18-19] and physical covering by surfactants or elastomers,[20-22] are employed to minimize interfacial energy and improve silica dispersion. These treatments also result in the destruction of surface silanol groups, which may act as reactive sites for interfacial reactions. To further enhance interfacial contact, surface functionalization using interfacial modifiers based on reactions with surface silanol groups is frequently employed. In styrene-butadiene rubber (SBR) nanocomposites, silica added with an interface crosslinker exhibits increased reinforcing efficiency.[23] Silane coupling agents like bis-(triethoxysilylpropyl)-tetrasulfide (TESPT), which generate covalent bonds between silica and the rubber matrix, have been shown to be efficient in-situ modifiers for rubber/silica composites.[24-26] This is because they can strengthen the interface. However, the interfacial modifier only slightly improves silica dispersion.[26] Consequently, poor silica dispersion reduces the amount of silica that the modifier can reach, resulting in an insufficient interfacial reaction.

The surface chemistry of silica can be gently changed to considerably increase silica dispersion, which improves the interface and the performance of rubber composites, according to Zhang *et al*.[27] Nevertheless, conventional silica alteration typically demands a lot of energy and takes a while to complete.[27-30] In actuality, another important factor for the functionalization of silica is the effectiveness of the surface reaction. To achieve fine control over the surface chemistry of silica, it is important to look for an effective yet straightforward technique.

With the aid of tris(pentafluorophenyl)borane (BCF) as a catalyst, a unique modification procedure for silica is carried out in this contribution.[31] It is based on the reaction between Si-H and silanol groups and may be finished at room temperature in a short amount of time. The reaction between silanol groups and Si-H, which is the basis of this procedure, can be accomplished in a short period of time at room temperature with BCF acting as a catalyst. As a result of this chemical functionalization technique, polymethylhydrosiloxane (PMHS) containing pendent Si-H groups can be grafted onto silica surfaces with ease. Considering the remaining Si-H bonds, it is envisaged that the grafted PMHS moiety will maintain reactivity and provide modified silica with reduced interfacial energy. Rubber was supplemented with PMHS-modified silicas of varying grafting contents to investigate the impact of the grafted PMHS on the dispersibility of silica nanoparticles and the interface between silica nanoparticles and the polymer matrix.

In the present work, the cure behavior, mechanical characteristics, abrasion resistance, swelling resistance, compression set, and morphological study of modified nanosilica filler-filled 50/50 EPDM/NBR nanocomposites were examined.

Experimental

Materials. The EPDM used was KEP-270 from the Swastik Group of Companies in Ahmedabad, Gujarat, India (Mooney viscosity, (ML1+4, 125 ℃) is 71 ± 6, ethylene is 56.5 wt%, ethylidene norbornene (ENB) content is 4.5 wt%, volatile content is 0.75% (maximum), specific gravity is 0.86, and propylene content is 38.25%). NBR of the JSR N230SL grade, with a 35% acrylontrile content and a 42 ± 1 Money viscosity (ML1+4, 100 ℃), was utilised. It was obtained from Hind Elastomers Pvt. Ltd. in Mumbai, India. The EPDM-grafted maleic anhydride (EPDM-g-MA) compatibilizer is available from Songhan Plastic Technology Co. Ltd., Shanghai City, China, and has the following specifications: maleic anhydride (MAH) content of 1%, Bondyram® 7001 trademark, propylene/ethylene ratio of 45/55, Mooney viscosity of ML (1 + 4) at 100 ℃ of 56 ± 2, and melt flow rate of 7 g/10 min. Vignesh Chemicals provided the curing system (stearic acid, ZnO, TMTD (tetramethylthiuram disulfide), and MBTS (benzothiazyl disulfide)), among other ingredients (Chennai, India). Hexane, heptane, HCL, octane, pentane, NaOH, toluene, ethanol, xylene, H_2SO_4, benzene, PMHS, mesitylene, chloroform, BCF, carbon tetrachloride, cyclohexylamine and dichloromethane were all of Merck grade were obtained from Sigma-Aldrich, Puducherry, India. To serve as a source of silica for the chemical synthesis of nanosilica particles, the rice husk (RH) was bought from a local mill.

Rice Husk Ash Preparation. Some rice grains and sand fragments are present in the obtained RH. To separate the rice grains from the husk, the material was repeatedly washed in tap water and then left to dry for 24 hours in the sun. The RH was then burned for three hours at 400 ℃ before being allowed to cool for twelve hours. After that, the ash was ground into tiny particles.[32] Figure 1 shows the preparation of rice husk ash.

Preparation of Silica Particles from RH Ash (RHA). 100 g of the cleaned RHA was refluxed for an hour at 70 ℃ with 800 mL of 2N HCl to remove metallic impurities. After the reaction was complete, the RHA was repeatedly washed in distilled water to remove the acid using filter paper with a pore size of 0.45 μm. After that, it was dried for 6 hours at 50 ℃ in an electric oven. After treatment, carbonaceous materials were eliminated from the treated RHA by heating it in an electrical box furnace for three hours at a temperature of 650 ℃ at a rate of 10 ℃ per minute, followed by furnace cooling. This process achieved white silica with high purity. While RHA that has undergone a 650 ℃ heat treatment is white, rice husk ash that has undergone a 400 ℃ heat treatment is black. Figure 1 also demonstrates the preparation of silica particles from rice husk ash.

Preparation of Silica Nanoparticles from Extracted Silica. Figure 2 shows the preparation of silica nanoparticles from extracted silica. 10 g of the obtained silica was refluxed with 80 mL of (6N) HCl for three hours at 65 ℃. Following the

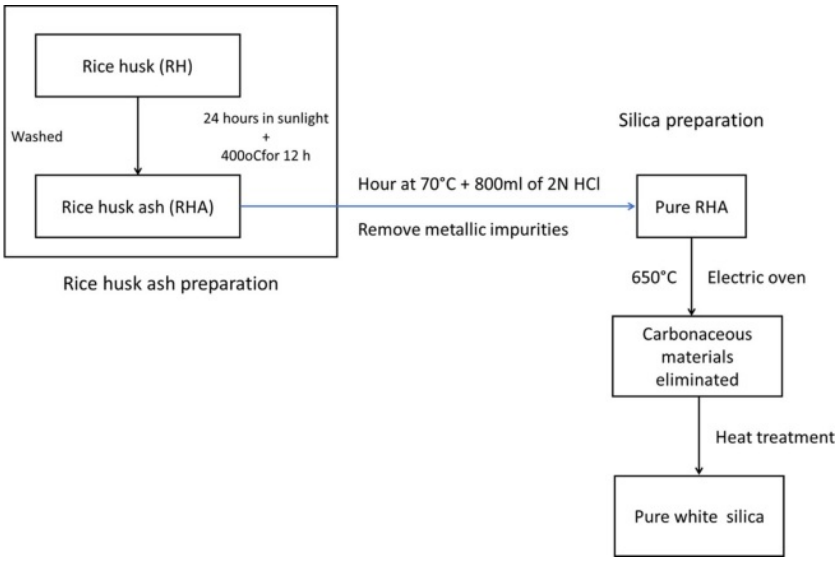

Figure 1. Preparation of rice husk ash and silica.

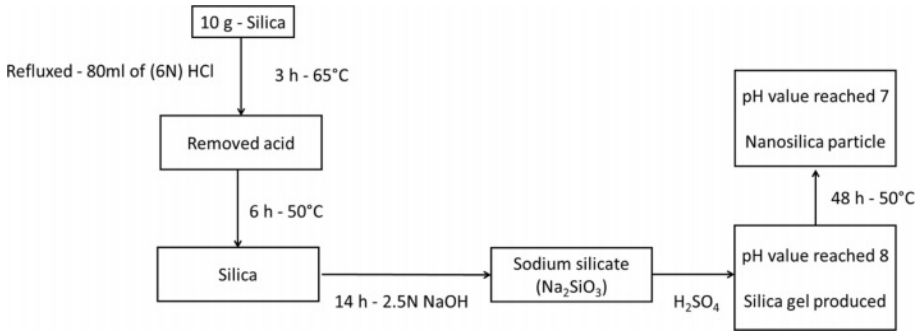

Figure 2. Flowchart of silica nanoparticles preparation from extracted silica.

completion of the reaction, the silica was cleaned with distilled water three times to remove the acid, and it was then vacuum-filtered using filter paper with a pore size of 0.2 μm. The silica was dried for six hours in an electric oven set to 50 ℃. To create sodium silicate (Na_2SiO_3), the silica was next magnetically agitated for 14 hours with a 2.5N NaOH solution. The pH was then steadily increased by adding H_2SO_4 to the Na_2SiO_3 solution until it reached 8, at which time a nanosilica gel was produced. The gel was then dried at 50 ℃ for 48 hours to produce the nanosilica particle powder after being washed in double-distilled water until the pH reached 7. According to the findings of the field emission-scanning electron microscopy (FESEM) analysis, the nanosilica was produced with a particle size of 30-50 nm and was almost spherical in shape, as shown in Figure 3.

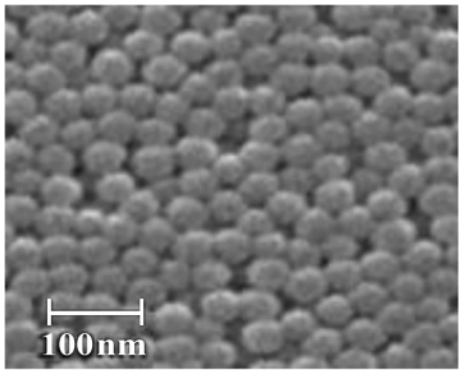

Figure 3. FESEM images of nanosilica.

Preparation of PMHS-modified Silica. Prior to modification, silica was dried under vacuum at 160 ℃ to eliminate absorbed water. In a flask, the dry silica was combined with toluene (25 mg/mL), followed by gradually higher concentrations of PMHS and BCF. When BCF was added, hydrogen evolution was clearly observable, demonstrating that the reaction had occurred. The alteration process took 15 minutes to complete at room temperature. Toluene and ethanol were used to fully clean the product, which was then vacuum-dried at 50 ℃ overnight. The ratio of PMHS to BCF in the mixture is kept constant (1.5:1 PMHS:BCF) to diversify the proportion of grafted PMHS on silica. Toluene was typically dissolved in 100 mL of 0.099 g (1 mmol) cyclohexylamine, 2 mL of water,

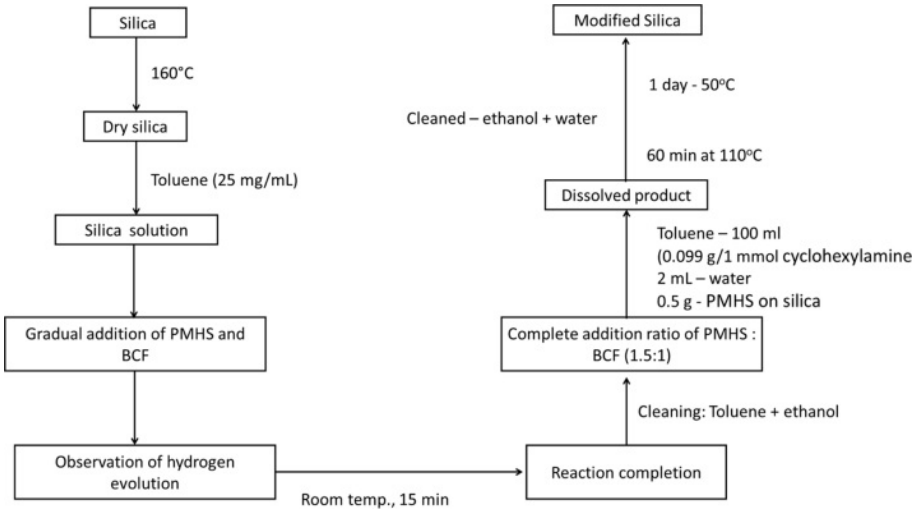

Figure 4. Workflow of PMHS-modified silica preparation.

Table 1. Formulations of EPDM/NBR-modified Nanosilica Nano-composites

Sample ID	EPDM	NBR	EPDM-g-MA	Pristine SiO_2	Modified SiO_2	ZnO	SA	Sul	MBTS	TMTD
EN_{50}-NS_0	50	50	5	0	-	4	1.5	2.5	1.2	1
EN_{50}-NS_2	50	50	5	2	-	4	1.5	2.5	1.2	1
EN_{50}-NS_4	50	50	5	4	-	4	1.5	2.5	1.2	1
EN_{50}-NS_6	50	50	5	6	-	4	1.5	2.5	1.2	1
EN_{50}-NS_8	50	50	5	8	-	4	1.5	2.5	1.2	1
EN_{50}-NS_{10}	50	50	5	10	-	4	1.5	2.5	1.2	1
EN_{50}-mNS_2	50	50	5	-	2	4	1.5	2.5	1.2	1
EN_{50}-mNS_4	50	50	5	-	4	4	1.5	2.5	1.2	1
EN_{50}-mNS_6	50	50	5	-	6	4	1.5	2.5	1.2	1
EN_{50}-mNS_8	50	50	5	-	8	4	1.5	2.5	1.2	1
EN_{50}-mNS_{10}	50	50	5	-	10	4	1.5	2.5	1.2	1

and 0.5 g of prepared material (grafted PMHS on silica). After being heated for 60 minutes at 110 ℃, the product was thoroughly cleaned many times with ethanol and water before being dried at 50 ℃ under vacuum for the day. Figure 4 shows the preparation of PMHS-modified silica.

Preparation of Rubber Blend Nanocomposites. The two-roll mill was used to create the rubber blends according to the formula in Table 1. Initially, NBR was added and mixed in a two-roll mill for three minutes. The compatibilizer EPDM-g-MA was then added, and mixing proceeded for a further two minutes. Finally, EPDM was added as the second rubber phase to the entire mixture. After 8 minutes of mixing, the sample was taken out and collected for further research. Once the NBR/EPDM-g-MA/EPDM-modified nanosilica (mNS) nanocomposite was created, the sample was produced using a two-roll mill for 5 minutes at room temperature. After that, ZnO and stearic acid were added to the system for two minutes. Subsequently, the system was supplemented with a curing system incorporating accelerators (MBTS, TMTD), and sulfur was added. The rubber compositions were then thermocompressed at 170 ℃ and molded into 2 mm-thick sheets. An oscillating disc curemeter was used to gauge the thermocompression cure time. For simplicity, the composites filled with 2 phr of mNS are designated by the sample code EN_{50}-mNS_2. Similar steps were taken to make the unfilled EPDM/NBR composite without adding silica.

Characterization. The polarity of the surface was examined through an immersion test. To conduct the test, a small amount of filler was placed on top of water, which served as the solvent. The original nanosilicas sank right away due to their

Table 2. Compression Set for EPDM/SBR-SiO_2 Composites

Sample ID	For 24 hours at 23 ℃	For 48 hours at 23 ℃	For 72 hours at 23 ℃	For 24 hours at 70 ℃	For 24 hours at 100 ℃
EN_{50}-NS_0	3.95	8.12	11.45	17.12	20.57
EN_{50}-NS_2	4.21	8.69	12.68	19.54	24.23
EN_{50}-NS_4	4.54	9.56	13.54	23.14	26.58
EN_{50}-NS_6	5.17	10.78	15.87	24.74	29.14
EN_{50}-NS_8	5.84	11.54	16.74	25.68	30.97
EN_{50}-NS_{10}	6.12	11.88	17.56	27.26	33.14
EN_{50}-mNS_2	4.36	8.87	13.54	20.15	25.21
EN_{50}-mNS_4	4.94	9.85	14.82	21.87	28.79
EN_{50}-mNS_6	5.98	11.17	16.27	25.45	30.58
EN_{50}-mNS_8	6.15	12.24	17.84	27.56	32.56
EN_{50}-mNS_{10}	6.48	12.85	19.54	28.79	35.83

hydrophilic surfaces; however, the modified fillers were expected to float for a longer period of time. To obtain more precise data on water penetration, it was necessary to seal the aperture of a glass column containing 0.02 g of filler with two layers of a hydrophobic filter with a pore size of 0.2 μm. This test aimed to monitor the weight change caused by the water's absorption over time as it was poured into the column.

The cure qualities were evaluated on an oscillating disc rheometer (ODR). The cure parameters of the various nanocomposites were examined using TechPro Rheotech ODR, and they are shown in Table 2 as follows: CRI - cure rate index; t_{90} - optimal cure time; t_{s2} - scorch time; M_l - minimum torque; M_h - maximum torque; and ΔM - delta torque (as per ASTM D-2084).

The ASTM D 412 standard was used to determine the tensile strength (TS), 100% modulus (M100), and percentage of elongation at break (EB%). Diverse mechanical parameters were accurately assessed using a universal testing equipment from Dak System Inc., which was equipped with programming and operated at a 500 mm/min crosshead speed. The samples were dumbbell-shaped, measuring 50 mm in length and 4 mm in width. Each recorded data point represents the average of five different outcomes. The experimental setup and tools used for tensile testing were also applied to the tear measurements. Test pieces at a 90° angle were used to measure tear strength (N/mm) following the guidelines of ASTM D-624.[33]

Flat-surfaced nanocomposites that were at least 10 mm thick were cut for the hardness test. The estimation was performed using a Model 306L class A Durometer, ASTM D 2240. The hardness unit is expressed in Shore A.[34]

The rebound resilience test for EPDM/NBR rubber composites was conducted following ASTM D 2632 guidelines. This technique involved releasing a plunger suspended at a predetermined height (400 mm) above the specimen and measuring the resulting rebound height. The ratio between the initial height and the rebound height, expressed as a percentage, defines the rebound resilience. The vertical rebound tester was employed as the resiliometer for the test, and each sample's mean of five measurements is presented.[35]

According to ASTM D5963, the DIN abrader was used to assess the abrasion resistance of EPDM/NBR rubber nanocomposites in terms of volume loss. The specimen, which had a cylindrical shape with measurements of 12 ± 0.2 mm in thickness and 10 ± 0.2 mm in diameter, was placed at the beginning position of the DIN abrader testing equipment. The specimen was then moved along at a constant velocity of 0.32 m/s and a constant force of 10 N, respectively, while being abrasively rubbed against grade 60 emery paper. When a 40-meter abraded distance was attained, the test specimen was mechanically raised off the DIN abrader emery paper. Equation [$(\Delta m \times S0)/(\rho \times S)$] was used to compute the rubber nanocomposites' abrasion loss or DIN volume loss, where Δm represents the mass loss in units of mg, ρ is the density in units of mg/mm^3, S_0 is the nominal abrasive power (value: 200 and unit: mg), and S is the average abrasive power in units of mg. The average value from a minimum of five tested and documented specimens was used to quantify the amount of abrasion loss for each sample.

On cylindrical standard test samples with a 12.5 ± 0.5 mm thickness and 12.5 ± 0.1 mm diameter, ASTM D 395's compression set test was performed. To allow enough room for elastic protrusion when packed, the test samples were placed between the compression set device's plates with slip gauge spacers on either side of them. The bolts were tightened to prevent the plates from moving apart until they came into contact with the spacers. After assembling the compression set device, it was put in an air-circulated oven preheated to 70 ℃ for 22 hours. Subsequently, the compression set test samples were taken out and given 30 minutes to cool. An electronic digital caliper evaluated the most recent thickness with ± 0.01 mm precision. The percentage of compression set is calculated using the formula $C\% = (t_o - t_1) / (t_o - t_s) \times 100$, where t_o is the sample's initial thickness, t_1 is its thickness after being released from the clamp, and t_s is the thickness of the spacer bar that was utilized.

Using the immersion method for the ASTM D471 swelling test, a sample of the vulcanized sheet measuring 25 × 25 × 2 mm^3 was cut from it. The sample was then dried in a vacuum desiccator for 24 hours. The specimen was rounded at the corners for homogeneous absorption. The test sample's thickness was measured with a digital Vernier caliper, which had a ± 0.01 mm accuracy. The specimen's initial weight was determined, and it was fully submerged in glass diffusion bottles containing aromatic (toluene, benzene, mesitylene, and xylene), aliphatic (n-hexane, -pentane, -octane, and -heptane), and chlorinated penetrants (dichloromethane, carbon tetrachloride, and chloroform). The samples were taken out of the glass diffusion bottles on a regular basis, cleaned with tissue paper, and subsequently weighed using an extremely sensitive electronic scale (± 0.001 g). The glass diffusion bottles were then refilled with the samples. The procedure was carried out several times until equilibrium swelling was reached. Using the formula [Q_t (mol%) = $\frac{(P_t - P_0)/MW}{P_0}$

× 100], the mole percent uptake Q_t for the penetrant/solvent was premeditated. Where P_0 is the sample's initial mass, P_t is the mass after 72 hours of entanglement, and MW is the solvent molecular weight.[36]

Using FESEM, the shape of the shattered surface resulting from the tensile test at a 3 kV acceleration voltage, coated with a gold layer, was examined (Hitachi S4160, made in Japan).

Results and Discussion

Filler Characterization. The hydrophobicity was tested by submersion in water to observe any changes. As predicted, the unprocessed mNS instantly sank to the bottom of the water, while some of the compound floated on the water for a considerable amount of time due to its behavior. This shows the decrease in polarity of the mNS following surface modification, but it also indicates an uneven coating that might have been caused by the inclusion of filler aggregates during the surface modification process. Figure 5 displays the results of water absorption. Over time, water was absorbed by both unmodified and mNS, eventually reaching an equilibrium level. However, since pure NS absorbed more water than mNS did, it indicates that mNS is more hydrophobic. The results of this preliminary study suggest that mNS might function more effectively with a rubber matrix material since they are less polar and more hydrophobic than the unmodified filler.

Cure Behaviors. Figure 6(a)-(f) clearly illustrates the curing properties of several compounds, including the following parameters: M_l - minimum rheometric torque, M_h - maximum rheometric torque, M_h-M_l - delta rheometric torque, t_{s2} - scorch time, t_{90} - optimum cure time, and CRI - cure rate index. The curing behaviors of EPDM/NBR rubber nanocomposites are influenced by the filler content and its surface characteristics.[37] The M_l, M_h, and M_h-M_l of the nanosilica-filled EPDM/NBR nanocomposites are shown in Figures 6(a) to 6(c). It has been reported that the M_l, M_h, and M_h-M_l of nanosilica-filled EPDM/NBR nanocomposites increase with increasing nanosilica loading, resulting from the curatives' adsorption by silica nanoparticles.[38] The processing parameters of the nanocomposites made of EPDM/NBR-nanosilica and the nanosilica dispersion were used to express the M_l value. The growing agglomerates of nanosilica give the EPDM/NBR nanocomposite the highest M_l. However, the M_l of EPDM/NBR nanocomposites reduced substantially, and to a greater extent, when modified extracted nanosilica (mNS) was used. This is because mNS breaks down agglomerates, leading to significantly higher M_h in mNS-EPDM/NBR nanocomposites compared to NS filler-filled-EPDM/NBR nanocomposites. The cross-linking between the EPDM/NBR matrix and the reinforcing material is indicated by the M_h-M_l. This suggests that the alteration causes fewer silanol groups to form on the surface of nanosilica, preventing the vulcanization reaction's adsorption of curatives. Moreover, as seen in Figure 14, this will result in a larger crosslink density.

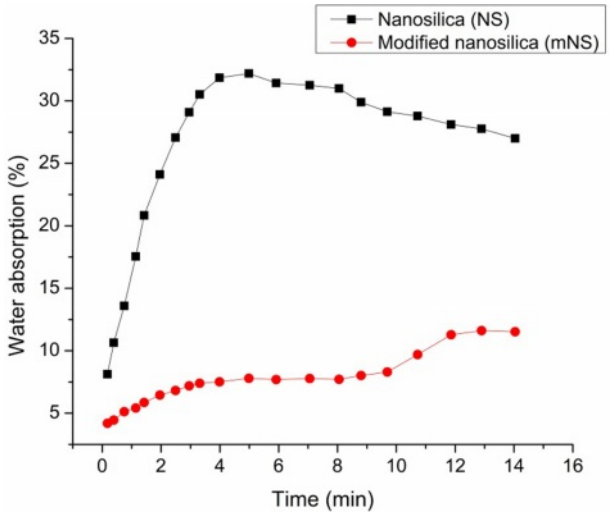

Figure 5. Water absorption of the modified nanosilica.

The diagram of the EPDM/NBR-nanosilica nanocomposites for t_{s2}, t_{90}, and CRI is shown in Figure 6(d)-(f). The vulcanization rate of the composite can be calculated using t_{s2} and t_{90}. The t_{s2} and t_{90} of the nanocomposites decrease as the concentration of nanosilica rises. This reduction is caused by the interaction of its ethoxy-groups with the surface of nanosilica. Additionally, the strong polar interaction between nanosilica and ZnO_2 during the vulcanization process, along with the production of ZnO_2 bound nanosilica, contributes to the decrease in t_{s2} and t_{90}. In the course of the vulcanization process, ZnO_2 activity is reduced to increase the accelerator.[39] At higher nanosilica content, the CRI of the nanocomposite EPDM/NBR filled with nanosilica increases. The hydroxyl group on the surface of the nanosilica effectively reacts with the silane and ethoxy groups, resulting in this effect. In the case of mNS, t_{s2} and t_{90} decrease while the CRI for the composites increases. The mNS nanoparticles exhibit a scorchy nature, as evidenced by the low scorch time data. The enhanced level of curing observed in EPDM/NBR nanocomposites with a higher proportion of mNS is attributed to the presence of a crosslinked system.

Mechanical Properties. In the vulcanizing press, the compounds were vulcanized to t_{90}, and afterward, their mechanical properties were evaluated. Figure 7(a)-(d) illustrates the mechan-

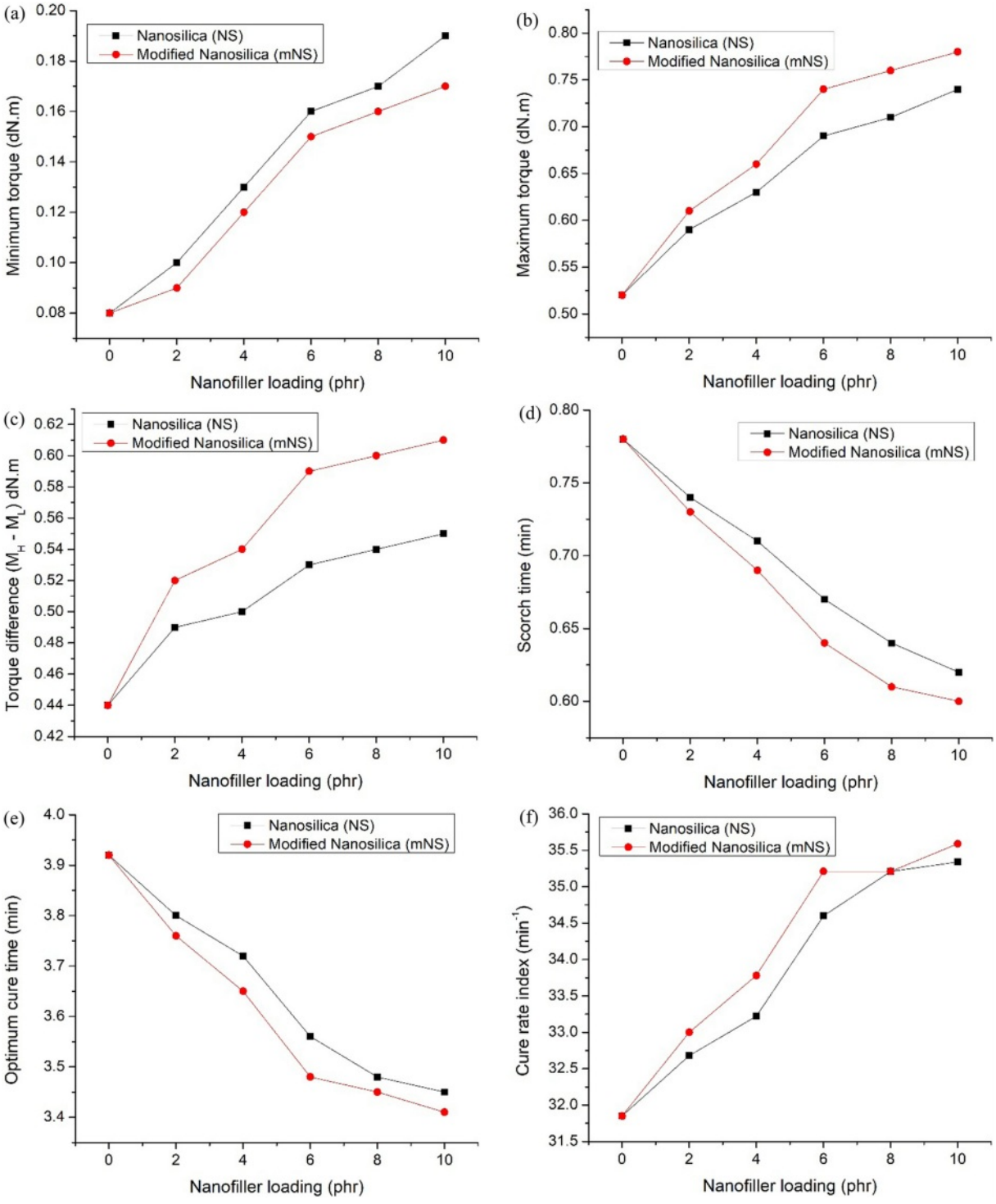

Figure 6. Cure characteristics of the nanosilica-EPDM/NBR nanocomposites: (a) M_l of the nanosilica-EPDM/NBR nanocomposites; (b) M_h of the nanosilica-EPDM/NBR nanocomposites; (c) M_h–M_l of the nanosilica-EPDM/NBR nanocomposites; (d) T_{s2} of the nanosilica-EPDM/NBR nanocomposites; (e) T_{90} of the nanosilica-EPDM/NBR nanocomposites; (f) CRI of the nanosilica-EPDM/NBR nanocomposites

ical attributes. Figure 7(a) depicts the tensile strength (TS) of EPDM/NBR composites filled with nanosilica filler. Up to 6 phr, the nanosilica concentration in EPDM/NBR nanocomposites causes a TS enhancement, which then steadily declines after that. The hydrophilic characteristic of silica nanoparticles, which results in the development of aggregates under higher

loading conditions, may be to blame for the poor nanosilica-EPDM/NBR interaction. Because of the formation of hydrogen bonds between the surface of the nanosilica and the silanol groups, there are more agglomerates and a non-uniform dispersion of the silica nanoparticles in the EPDM/NBR rubber matrix. The TS of the EPDM/NBR nanocomposites including mNS increased by 8% compared to the EPDM/NBR nanocomposites with immaculate nanosilica and by 51% compared to gum rubber. The incorporation of mNS improved the TS because most of the silanol groups on the surface of the NS reacted with the NS particles to make them compatible with the rubber blend (EPDM/NBR) and became evenly disseminated within it. The elongation at break (EB) and modulus at 100% (M100) of EPDM/NBR composites are shown in Figures 7(b) and (c), respectively. In EPDM/NBR rubber nanocomposites, the EB and M100 rise with increasing nanosilica loading up to a phr of 6 and fall with additional loading. The increase in EB is a sign of effective wetting of the nanosilica and a strong filler-rubber interfacial adhesion. The reduction in EB is a sign that polymeric molecular chains are restricted in their ability to move. The M100 of the EPDM/NBR composites was influenced by the loading of nanosilica concentration and the size of particles.[40] When compared to a nanocomposite made of pristine nanosilica, the EPDM/NBR nanocomposites with mNS exhibit a 4% reduction in EB and a 6% rise in M100. In comparison to neat rubber, the EB and M100 of the nanocomposites with mNS are increased by 12% and 23%, respectively. Figure 7(d) displays the tear strength (TAS) of EPDM/NBR nanocomposites. As the loading of NS in the EPDM/NBR increases, the TAS of the rubber nanocomposite also increases. Compared to EPDM/NBR nanocomposite made with pristine nanosilica, the mNS variant of the material had greater tear

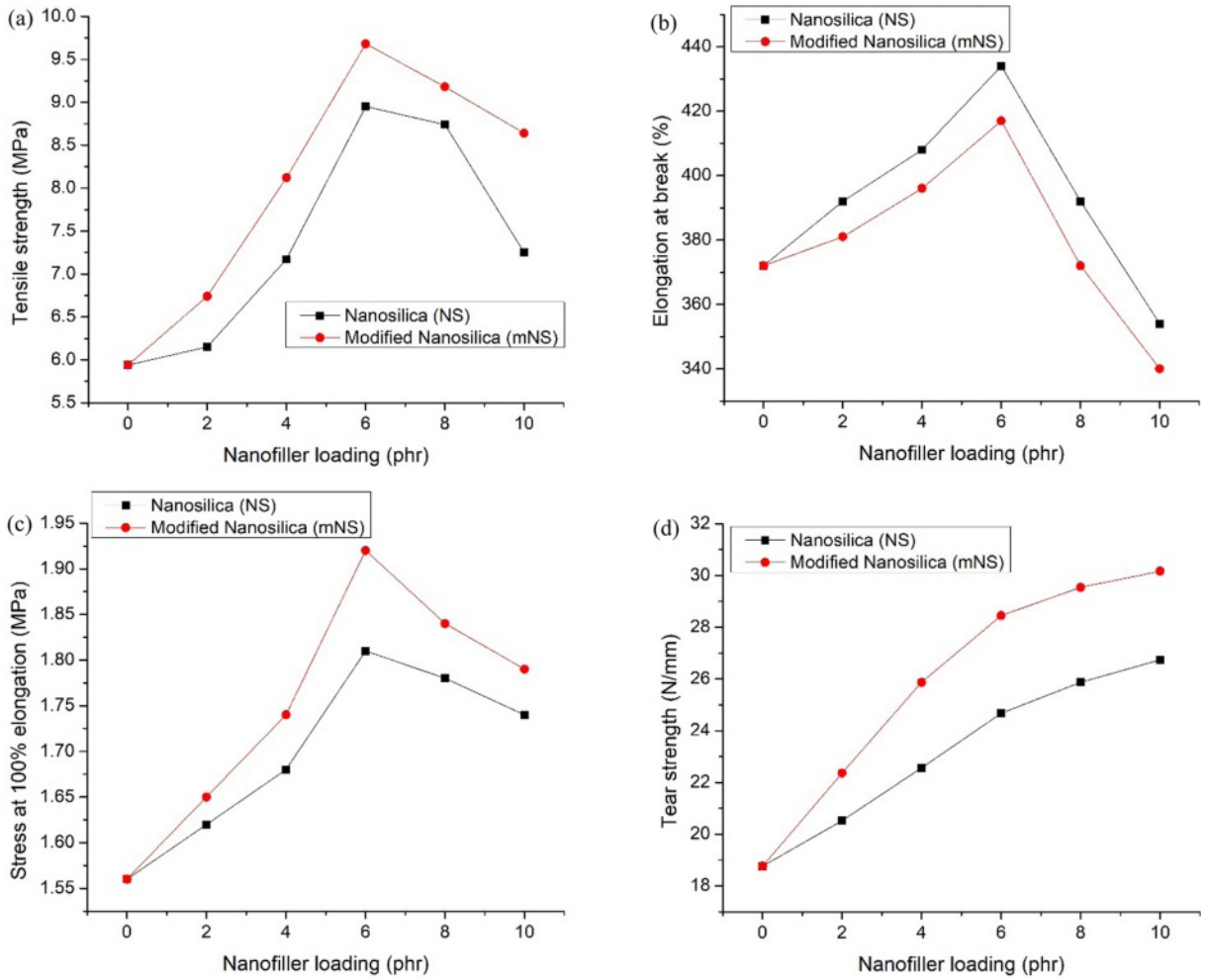

Figure 7. Mechanical characteristics of the nanosilica-EPDM/NBR nanocomposites: (a) tensile strength of the nanosilica-EPDM/NBR nanocomposites; (b) elongation at break of the nanosilica-EPDM/NBR nanocomposites; (c) 100% modulus of the nanosilica-EPDM/NBR nanocomposites; (d) tear strength of the nanosilica-EPDM/NBR nanocomposites

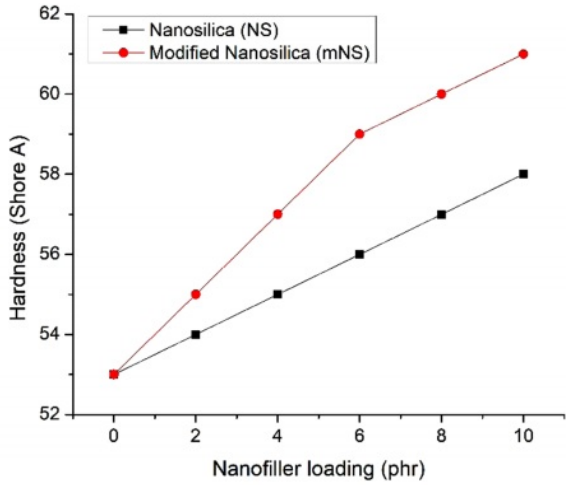

Figure 8. Hardness of the nanosilica filler filled EPDM/NBR nanocomposites.

strength. This resulted from the rubber nanocomposite's increased crosslink density.

The hardness of nanosilica-EPDM/NBR composites is depicted in Figure 8. The nanosilica-EPDM/NBR composite becomes harder as the nanosilica concentration rises. The EPDM/NBR-SiO_2 composite with mNS shows that the increase in hardness was brought on by a higher crosslink density and improved silica dispersion. The improved hardness was caused by a higher crosslinking density. The composite's softer matrix becomes tougher as the crosslink density rises. Figure 9 displays the composites' rebound resilience. The stiffness and rigidity of EPDM/NBR composites are simultaneously improved when the concentration of nanosilica rises, while the rebound resilience falls. Due to the negative correlation with the material's hardness, the nanocomposite's rebound resilience dropped as the concentration of nanosilica increased. The addition of nanosilica caused a decrease in rebound resilience because it increased the reinforcing effect.[41] A better EPDM/NBR-nanosilica interaction may be to blame for the decline in the propensity of rebound resilience. EPDM/NBR composites with and without mNS have comparable rebound resilience. As the amount of NS particles in the EPDM/NBR matrix increased, the elasticity of the polymer chains decreased, resulting in low rebound resilience.[42] The conversion of energy used into heat lowers the EPDM/NBR composite's rebound resilience. In general, it can be said that the amount of heat buildup during the operation was inversely proportional to the rubber composite's resilience.[43]

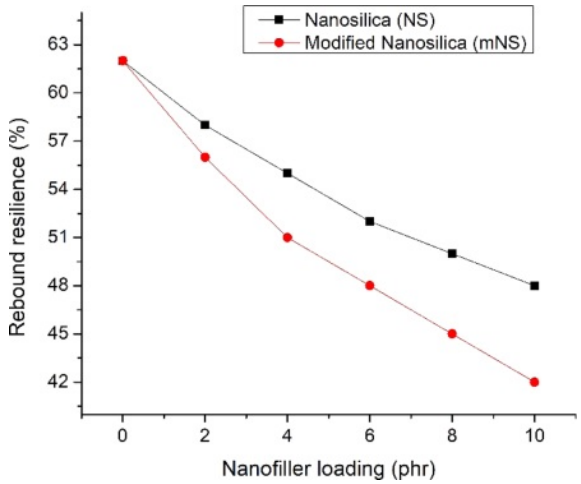

Figure 9. Rebound resilience of the nanosilica filler filled EPDM/NBR nanocomposites.

Abrasion Resistance. Abrasion resistance was a key factor to consider while assessing the rubber material's service life. During the DIN test, the volume loss was used to measure it.[44] The abrasion loss of the EPDM/NBR rubber blend nanocomposites was exposed in Figure 10. Composite materials become increasingly abrasion-resistant as the nanosilica concentration rises. At a specific nanosilica loading, mNS-containing composites had a clearly higher abrasion resistance than those without mNS. The increased abrasion resistance property may result from the more even distribution of nanosilica in the EPDM/NBR rubber matrix. It is clear from the decreased abrasion loss in the EPDM/NBR composites that the nanosilica used as the reinforcing material has a better interfacial contact with the matrix of EPDM/NBR.

Compression Set. The compression set values for the composites are shown in Table 2. As indicated in Table 2, the compression set for regular rubber is moderate, but it increases

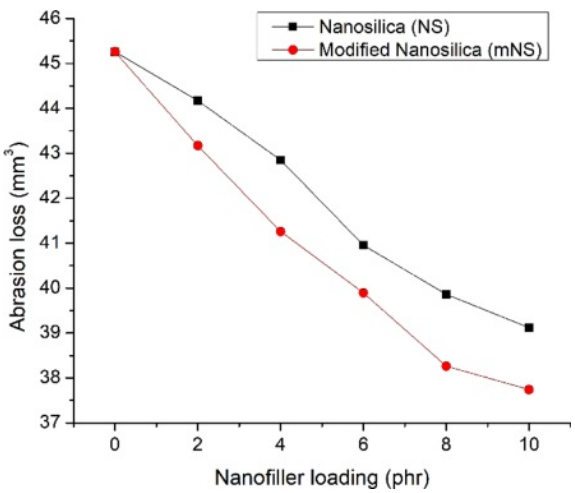

Figure 10. Abrasion loss of the EPDM/NBR-SiO_2 composites.

in parallel with a rise in the concentration of nanosilica. As the modulus of composites increased, the rubber chain's mobility remained restricted even after the applied force had been removed. The cross-link density and the compression set percentage value of the nanocomposite likewise increase as the concentration of nanosilica does, while the mobility of the polymer chains decreases, making the composites stiffer. Increases in cross-linking density produce high compression set values, as would be predicted. When comparing EPDM/SBR-SiO_2 composites with mNS to composites filled with NS filler, the crosslinking density was somewhat higher in the mNS instance. The percentage of compression set increases with increasing time and temperature, and Table 2 clearly shows this relationship. The rubber material's capacity to set in compression is strongly influenced by temperature. A higher compression set is a sign that the rubber composite can still maintain some elastic properties, but they are less desirable. The better the composite material is for an engineering purpose, the lower the percentage of compression set.

Swelling Properties. The type of matrix, filler, geometry of the filler (size, size distribution, orientation, shape, and content), reaction between the rubber matrix and penetrant, penetrants, temperature, etc., all had an impact on the swelling behavior of the composites. Hence, the study of the composites' swelling properties can be used to understand the system's interfacial interaction. Rubbers are mostly utilized in industrial applications, and throughout their lifetime, they are subjected to various chemical conditions. Analysis was done on the impact of penetrant type and nanosilica loading on the mole percent uptake (MPU) through SiO_2-EPDM/NBR nanocomposites. The swelling curves were shown in Figures 11-13 and denoted

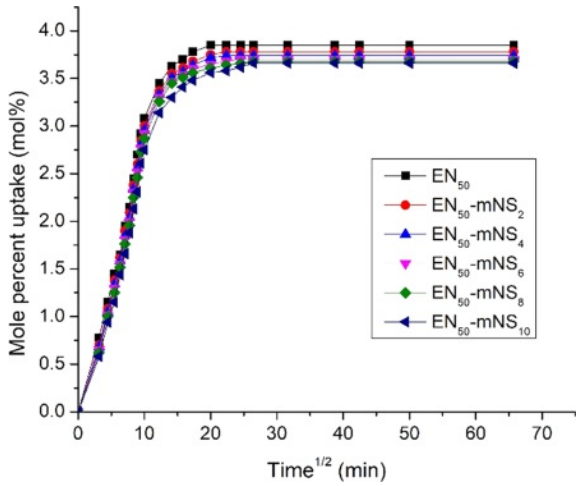

Figure 11. Mole percent uptake of toluene by nanosilica loading.

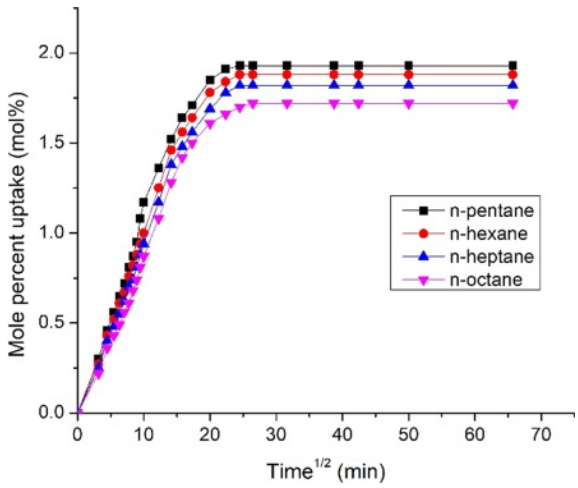

Figure 12. Mole percent uptake of aliphatic penetrants through 10 phr nanosilica filled EPDM/NBR composites.

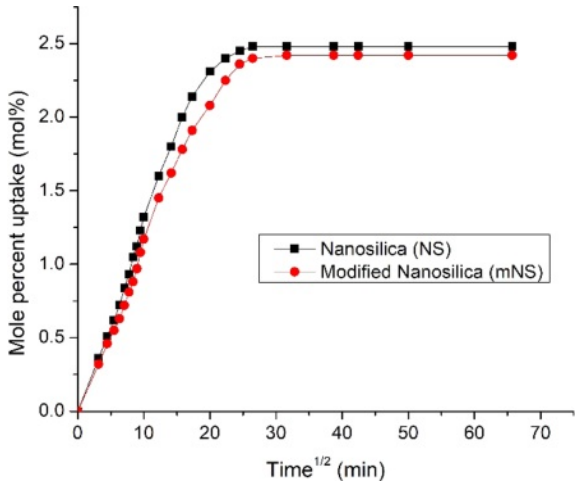

Figure 13. Mole percent uptake of chloroform through 10 phr treated and untreated nanosilica filled EPDM/NBR composites.

as a graph (*i.e.*, mole percent uptake (Q_t) of the composite vs. the square root of time ($t^{1/2}$)). Table 3 displays the swelling characteristics for various penetrants at various nanosilica loadings in SiO_2-EPDM/NBR composites in terms of MPU. The penetrants utilized are aliphatic penetrants (n-pentane, -hexane, -heptane, and -octane), aromatic penetrants (benzene, toluene, xylene, and mesitylene), as well as chlorinated penetrants (dichloromethane, chloroform, and carbon tetrachloride). Figure 11 clearly depicts the MPU of toluene by nanosilica loading. When the content of silica nanoparticles increases, the MPU of EPDM/NBR rubber blend nanocomposites filled with nanosilica declines. In actual fact, as the concentration of nanosilica rises, the crosslinking density in polymer nanocomposites also rises dramatically, increasing network elasticity. Additionally,

crosslinks reduce the amount of swelling and fight the propensity for dissolution by limiting the extensibility of the elastomeric chains (specifically, rubber/macro-molecular chains) caused by swelling and making it more difficult for the penetrant (solvent) to diffuse in the spaces between elastomeric material molecules.[45] As a result, swelling goes down as the network grows. According to Table 3, composites containing mNS in EPDM/NBR-SiO_2 had significantly better swelling characteristics than those with NS at a similar loading of nanosilica. This resulted from the increased crosslinking density of mNS-crosslinked EPDM/NBR-SiO_2 composites compared to NS-crosslinked composites. Thus, using aromatic, aliphatic, and chlorinated solvents led to a similar trend, as shown in Table 3.

Figure 12 shows the impact of penetrant size on the maximum possible uptake (MPU) of aliphatic penetrants through nanosilica particles filled EPDM/NBR nanocomposites at 10 phr. The solvent with a lower molecular weight exhibits the highest MPU for the EPDM/SBR rubber composite, whereas the solvent with a larger molecular weight exhibits the lowest MPU. As can be seen from Table 3, the trend was as follows: 1) aromatic penetrants: benzene (C_6H_6) > toluene (C_7H_8) > xylene (C_8H_{10}) > mesitylene (C_9H_{12}); 2) aliphatic penetrants: n-pentane (C_5H_{12}) > n-hexane (C_6H_{14}) > n-heptane (C_7H_{16}) > n-octane (C_8H_{18}); and 3) chlorinated penetrants: dichloromethane (CH_2Cl_2) > chloroform ($CHCl_3$) > carbon tetrachloride (CCl_4). As a result, the relationship between the molecular mass and solvent penetrant is inverse. Lastly, the composite's greater swelling suggests that it is unsuitable for use in industrial applications.

Figure 13 shows the impact of extracted nanosilica that has been treated and untreated on the MPU of chloroform through 10 phr nanosilica filler-filled EPDM/NBR nanocomposites. The solvent resistance of EPDM/NBR composites was improved by the incorporation of mNS. Hence, when compared to the composite containing NS (non-modified nanosilica), the mNS-EPDM/NBR composite with higher nanosilica loading was practically preferred for industrial application.

Crosslinking Density. Figure 14 displays the crosslinking density values for composites made of EPDM, NBR, and SiO_2. The crosslinking density was calculated using the swelling data. The crosslinking density (υ) of the nanocomposite increases

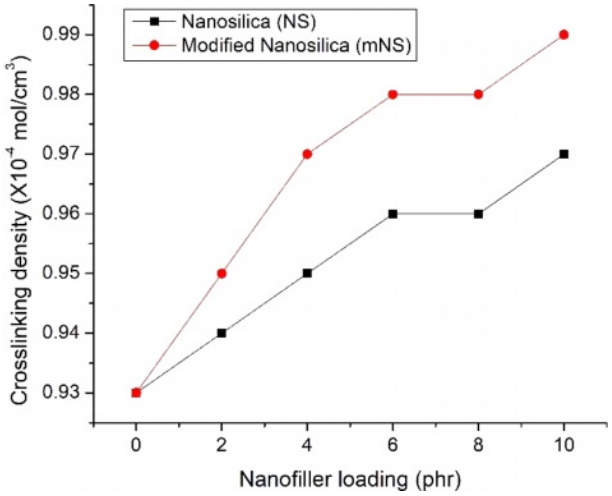

Figure 14. Crosslinking density of the EPDM/NBR-SiO_2 composites.

Table 3. MPU of Aromatic, Aliphatic and Chlorinated Penetrant of Nanosilica Filler Filled EPDM/NBR Nanocomposites

Sample ID (SID)	Mole percent uptake (MPU) (mol%)										
	Aromatic solvents				Aliphatic solvents				Chlorinated solvents		
	Benzene (C_6H_6)	Toluene (C_7H_8)	Xylene (C_8H_{10})	Mesitylene (C_9H_{12})	n-pentane (C_5H_{12})	n-hexane (C_6H_{14})	n-heptane (C_7H_{16})	n-octane (C_8H_{18})	Dichloromethane (CH_2Cl_2)	Chloroform ($CHCl_3$)	Carbon tetrachloride (CCl_4)
EN_{50}-NS_0	4.12	3.85	3.65	3.1	2.08	2.04	2.02	1.88	2.75	2.65	2.38
EN_{50}-NS_2	4.07	3.81	3.62	3.06	2.06	2.01	1.97	1.85	2.71	2.62	2.35
EN_{50}-NS_4	4.03	3.78	3.59	3.02	2.03	1.98	1.94	1.83	2.68	2.55	2.31
EN_{50}-NS_6	3.99	3.75	3.57	2.98	1.99	1.96	1.91	1.8	2.64	2.54	2.28
EN_{50}-NS_8	3.97	3.74	3.55	2.96	1.98	1.94	1.9	1.79	2.62	2.51	2.25
EN_{50}-NS_{10}	3.95	3.72	3.54	2.95	1.96	1.92	1.88	1.77	2.6	2.48	2.24
EN_{50}-mNS_2	4.04	3.78	3.57	3.02	2.04	1.98	1.94	1.83	2.7	2.6	2.32
EN_{50}-mNS_4	3.97	3.74	3.54	2.95	2.01	1.95	1.9	1.8	2.65	2.52	2.28
EN_{50}-mNS_6	3.91	3.7	3.48	2.9	1.96	1.92	1.86	1.76	2.61	2.48	2.24
EN_{50}-mNS_8	3.89	3.68	3.45	2.88	1.95	1.9	1.85	1.74	2.58	2.45	2.23
EN_{50}-mNS_{10}	3.87	3.66	3.44	2.85	1.93	1.88	1.82	1.72	2.55	2.42	2.21

with the concentration of nanosilica. A higher crosslinking density results in improved mechanical characteristics, hardness, swelling resistance, and abrasion resistance.[46,47]

Morphology. The definitive characteristics of EPDM/NBR rubber blend nanocomposites are determined by the distribution of nanoparticles in the polymer matrix. The characteristics of the EPDM/NBR rubber nanocomposite are improved by uniform nanofiller distribution. A stress concentration point is created by the aggregated nanofillers, which causes the characteristics of composite materials to decline.[48] The silica nanoparticle dispersion in the EPDM/NBR rubber matrix greatly affects the tensile performance of rubber nanocomposites. The morphology of the rubber nanocomposites on the tensile fracture surface is shown in Figure 15(a)-(d). According to Figure 15(a), even though the amount of nanosilica increased, the majority of the particles were still nanodispersed. In addition, the unmodified nanosilica particles diffuse unevenly with agglomerates in the rubber matrix due to the formation of hydrogen bonds between the silanol groups on the nanosilica surface. Contrarily, almost all of the silanol groups on the surface of the nanosilica were reacted after being altered, resulting in the nanosilica particles compacting with the EPDM/NBR matrix and becoming equally dispersed in EPDM/NBR nanocomposites, as demonstrated in Figure 15(b). In other words, PMHS might be the result of grafting nanosilica surfaces into the molecular chains of the rubber matrix, which improves the compatibility of the rubber matrix and nanofiller in the composite and subsequently promotes nanodispersion of nanosilica in the rubber matrix. Figure 15(b) shows a considerable improvement in the dispersion of SiO_2 nanoparticles in the EPDM/NBR matrix and a significant decrease in the size of silica nanoparticle agglomerates compared to Figure 15(a). This is one of the main causes of the improvement in mechanical properties.

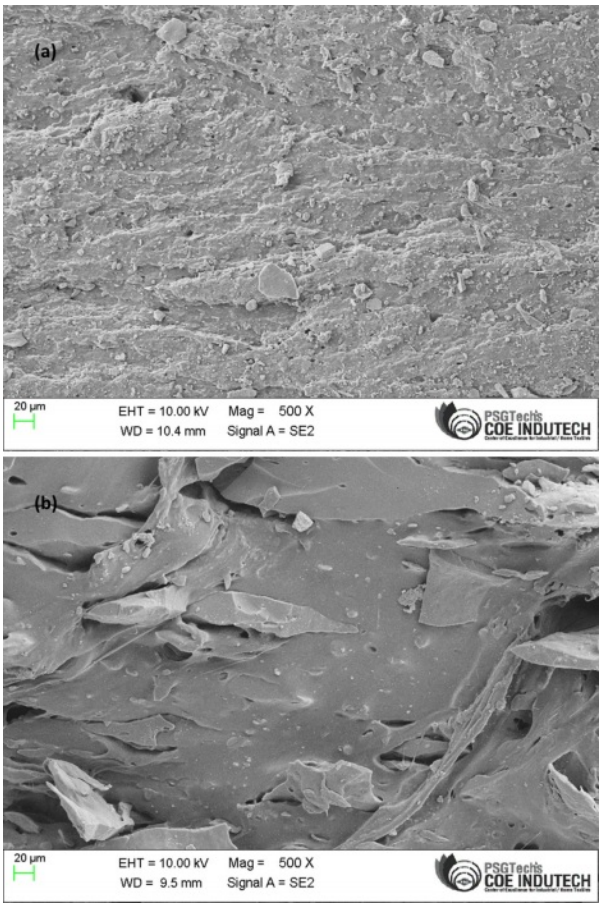

Figure 15. The tensile fractured surfaces with magnification X = 5 EN_{50}-mNS_6.

Conclusions

The curing behaviors, mechanical parameters, rebound resilience, hardness, compression set, abrasion, and swelling resistance of EPDM/NBR-nanosilica nanocomposites were examined and reported in the current investigations. The results of the experiment led to the following deductions: when the concentration of nanosilica in the EPDM/NBR-SiO_2 composites increases, t_{s2} and t_{90} drop, while the M_l, M_h, M_h-M_l, and CRI increase. According to the cure properties, nanosilica speeds up the curing process and strengthens the EPDM/NBR composites. The torque values for the nanosilica-loaded composites increased, which amply demonstrates the presence of more crosslinks in the system. Both EPDM/NBR-SiO_2 composites exhibit an increase in TS, EB, and M100 with increasing nanosilica concentration, up to 6 phr. With the addition of nanosilica particles, the rubber matrix's TAS, hardness, abrasion, and swelling resistance are all increased; however, the rebound resilience is diminished. The EPDM/NBR-SiO_2 nanocomposites with mNS had somewhat better mechanical characteristics, abrasion resistance, hardness, and swelling resistance than the composites with untreated extracted nanosilica at a similar nanosilica loading. This was because the EPDM/NBR-SiO_2 composites with mNS had a higher crosslinking density than the other composites.

Acknowledgements: The authors are highly grateful to SA Engineering college, Sri Eshwar College of Engineering, & Chennai Institute of Technology, Tamilnadu, India for their kind support in providing the time for research for academic interest.

Conflict of Interest: The authors declare that there is no conflict of interest.

References

1. Vishvanathperumal, S.; Navaneethakrishnan, V.; Anand, G.; Gopalakannan, S. Evaluation of Crosslink Density Using Material Constants of Ethylene-propylene-diene Monomer/styrene-butadiene Rubber with Different Nanoclay Loading: Finite Element Analysis-simulation and Experimental. *Adv. Sci., Eng. Med.* **2020**, 12, 632-642.
2. Anand, G.; Vishvanathperumal, S. Properties of SBR/NR Blend: The Effects of Carbon Black/Silica (CB/SiO_2) Hybrid Filler and Silane Coupling Agent. *Silicon* **2022**, 14, 9051-9060.
3. Dhanasekar, S.; Baskar, S.; Vishvanathperumal, S. Halloysite Nanotubes Effect on Cure and Mechanical Properties of EPDM/NBR Nanocomposites. *J. Inorg. Org. Polym. Mater.* 2023, 1-13.
4. Ragupathy, K.; Prabaharan, G.; Pragadish, N.; Vishvanathperumal, S. Effect of Silica Nanoparticles and Modified Silica Nanoparticles on the Mechanical and Swelling Properties of EPDM/SBR Blend Nanocomposites. *Silicon* **2023**, 1-14.
5. Das, R. K.; Ragupathy, K.; Kumar, T. S.; Vishvanathperumal, S. Effect of Halloysite Nanotubes (HNTs) on Mechanical Properties of EPDM/NBR Blend-Nanocomposites. *Polym. Korea* **2023**, 47, 221-232.
6. Ai, C.; Gong, G.; Zhao, X.; Liu, P. Determination of Carboxyl Content in Carboxylated Nitrile Butadiene Rubber (XNBR) After Degradation *via* Olefin Cross Metathesis. *Polym. Test.* **2017**, 60, 250-252.
7. Sundar, R.; Mohan, S. K.; Vishvanathperumal, S. Effect of Surface Modified Halloysite Nanotubes (mHNTs) on the Mechanical Properties and Swelling Resistance of EPDM/NBR Nanocomposites. *Polym. Korea* **2022**, 46, 728-743.
8. Doufnoune, R.; Haddaoui, N. Effects of Surface Functionalized Partially Reduced Graphene Oxide and Different Compatibilizers on the Properties and Structure of PP/EPR Nanocomposites. *J. Polym. Res.* **2017**, 24, 138-147.
9. Vishvanathperumal, S.; Anand, G. Effect of Nanoclay/nanosilica on the Mechanical Properties, Abrasion and Swelling Resistance of EPDM/SBR Composites. *Silicon* **2020**, 12, 1925-1941.
10. Vishvanathperumal, S.; Anand, G. Effect of Nanosilica and Crosslinking System on the Mechanical Properties and Swelling Resistance of EPDM/SBR Nanocomposites with and Without TESPT. *Silicon* **2021**, 13, 3473-3497.
11. Kueseng, P.; Sae-oui, P.; Rattanasom, N. Mechanical and Electrical Properties of Natural Rubber and Nitrile Rubber Blends Filled with Multi-wall Carbon Nanotube: Effect of Preparation Methods, *Polym. Test.* **2013**, 32, 731-738.
12. Chow, W. S.; Bakar, A. A.; Ishak, Z. M.; Karger-Kocsis, J.; Ishiaku, U. S. Effect of Maleic Anhydride-grafted Ethylene–propylene Rubber on the Mechanical, Rheological and Morphological Properties of Organoclay Reinforced Polyamide 6/polypropylene Nanocomposites. *Eur. Polym. J.* **2005**, 41, 687-696.
13. Bonilla-Cruz, J.; Hernández-Mireles, B.; Mendoza-Carrizales, R.; Ramírez-Leal, L. A.; Torres-Lubián, R.; RamosdeValle, L. F.; Paul, D. R.; Saldívar-Guerra, E. Chemical Modification of Butyl Rubber with Maleic Anhydride *via* Nitroxide Chemistry and Its Application in Polymer Blends. *Polymers* **2017**, 9, 63.
14. Azizli, M. J.; Mokhtary, M.; Khonakdar, H. A.; Goodarzi, V.; Hybrid Rubber Nanocomposites Based on XNBR/EPDM: Select the Best Dispersion Type from Different Nanofillers in the Presence of a Compatibilizer. *J. Inorg. Org. Polym. Mater.* **2020**, 30, 2533-2550.
15. Rafiee, E.; Shahebrahimi, S.; Feyzi, M.; Shaterzadeh, M. Optimization of Synthesis and Characterization of Nanosilica Produced from Rice Husk (a common waste material). *Int. Nano Lett.* **2012**, 2, 29.
16. Vishvanathperumal, S.; Navaneethakrishnan, V.; Gopalakannan, S. The Effect of Nanoclay and Hybrid Filler on Curing Characteristics, Mechanical Properties and Swelling Resistance of Ethylene-vinyl Acetate/styrene Butadiene Rubber Blend Composite. *J. Adv. Micros. Res.* **2018**, 13, 469-476.
17. Liu, Y.; Cao, L.; Yuan, D.; Chen, Y. Design of Super-tough Co-continuous PLA/NR/SiO_2 TPVs with Balanced Stiffness-toughness Based on Reinforced Rubber and Interfacial Compatibilization. *Compos. Sci. Technol.* **2018**, 165, 231-239.
18. Changwoon, N.; Mong-Young, H.; Rhee, J. M.; Tae-Ho, Y. Plasma Surface Modification of Silica and Its Effect on Properties of Styrene–butadiene Rubber Compound, *Polym. Int.* **2002**, 51, 510-518.
19. Shanmugharaj, A. M.; Bhowmick, A. K. Dynamic Mechanical Properties of Styrene-butadiene Rubber Vulcanizate Filled with Electron Beam Modified Surface-treated Dual-phase Filler, *J. Appl. Polym. Sci.* **2010**, 88, 2992-3004.
20. Lee, J. Y.; Lee, T.; Kim, K.; Kim, B.; Kwag, G.; Kim, J. Y.; Ji, S.; Kim, W.; Paik, H. J. Poly(styrene-r-butadiene)-b-poly(poly(ethylene glycol) methyl ether methacrylate) as a Silica Dispersant in Rubber Compounds, *Polym. Int.* **2014**, 63, 908-914.
21. Xu, T.; Jia, Z.; Luo, Y.; Jia, D.; Zheng, P. Interfacial Interaction Between the Epoxidized Natural Rubber and Silica in Natural Rubber/silica Composites, *Appl. Surface Sci.* **2015**, 328, 306-313.
22. Liu, Y.; Cao, L.; Yuan, D.; Chen, Y. Design of Super-tough Co-continuous PLA/NR/SiO_2 TPVs with Balanced Stiffness-toughness Based on Reinforced Rubber and Interfacial Compatibilization, *Compos. Sci. Technol.* **2018**, 165, 231-239.
23. Chen, L.; Jia, Z.; Tang, Y.; Wu, L.; Luo, Y.; Jia, D. Novel Functional Silica Nanoparticles for Rubber Vulcanization and Reinforcement, *Compos. Sci. Technol.* **2017**, 144, 11-17.
24. Castellano, M.; Conzatti, L.; Turturro, A.; Costa, G.; Busca, G. Influence of the Silane Modifiers on the Surface Thermodynamic Characteristics and Dispersion of the Silica Into Elastomer Compounds, *J. Phys. Chem. B* **2007**, 111, 4495-4502.
25. Kaewsakul, W.; Sahakaro, K.; Dierkes, W. K.; Noordermeer, J. W. Mechanistic Aspects of Silane Coupling Agents with Different Functionalities on Reinforcement of Silicafilled Natural Rubber

Compounds, *Polym. Eng. Sci.* **2015**, 55, 836-842.
26. Zheng, J.; Han, D.; Zhao, S.; Ye, X.; Wang, Y.; Wu, Y.; Dong, D. Liu, J.; Wu, X.; Zhang, L. Constructing a Multiple Covalent Interface and Isolating Disperion Structure in Silica/rubber Nanocomposites with Excellent Dynamic Performance, *ACS Appl. Mater. Interfaces* **2018**, 10, 19922-19931.
27. Zhang, C.; Tang, Z.; Guo, B.; Zhang, L. Significantly Improved Rubber-silica Interface *via* Subtly Controlling Surface Chemistry of Silica, *Compos. Sci. Technol.* **2018**, 156, 70-77.
28. Li, Y.; Han, B.; Wen, S.; Lu, Y.; Yang, H.; Zhang, L.; Liu, L. Effect of the Temperature on Surface Modification of Silica and Properties of Modified Silica Filled Rubber Composites, *Compos. Part A* **2014**, 62, 52-59.
29. Vansant, E. F.; Van Der Voort, P.; Vrancken, K. C. Characterization and Chemical Modification of the Silica Surface. *Elsevier* 1995.
30. Lin, J.; Chen, H.; Yuan, Y.; Ji, Y. Mechanochemically Conjugated PMHS/nano-SiO_2 Hybrid and Subsequent Optimum Grafting Density Study, *Appl. Surface Sci.* **2011**, 257, 9024-9032.
31. Moitra, N.; Ichii, S.; Kamei, T.; Kanamori, K.; Zhu, Y.; Takeda, K.; Nakanishi, K.; Shimada, T. Surface Functionalization of Silica by Si-H Activation of Hydrosilanes, *J. Am. Chem. Soc.* **2014**, 136, 11570-11573.
32. Vishvanathperumal, S.; Anand, G. Effect of Nanosilica on the Mechanical Properties, Compression Set, Morphology, Abrasion and Swelling Resistance of Sulphur Cured EPDM/SBR Composites. *Silicon* **2022**, 14, 3523-3534.
33. Ganeche, P. S.; Balasubramanian, P.; Vishvanathperumal, S. Halloysite Nanotubes (HNTs)-Filled Ethylene-Propylene-Diene Monomer/Styrene-Butadiene Rubber (EPDM/SBR) Composites: Mechanical, Swelling, and Morphological Properties. *Silicon* **2022**, 14, 6611-6620.
34. Vishvanathperumal, S.; Gopalakannan, S. Reinforcement of Ethylene Vinyl Acetate with Carbon Black/silica Hybrid Filler Composites. *Appl. Mech. Mater.* **2016**, 852, 16-22.
35. Senthilvel, K.; Vishvanathperumal, S.; Prabu, B.; John Baruch, L. Studies on the Morphology, Cure Characteristics and Mechanical Properties of Acrylonitrile Butadiene Rubber with Hybrid Filler (carbon black/silica) Composite. *Polym. Polym. Compos.* **2016**, 24, 473-480.
36. Vishvanathperumal, S.; Gopalakannan, S. Swelling Properties, Compression Set Behavior and Abrasion Resistance of Ethylene-propylene-diene Rubber/styrene Butadiene Rubber Blend Nanocomposites. *Polym. Korea* **2017**, 41, 433-442.
37. Zhang, C.; Tang, Z.; Guo, B.; Zhang, L. Significantly Improved Rubber-silica Interface *via* Subtly Controlling Surface Chemistry of Silica. *Compos. Sci. Technol.* **2018**, 156, 70-77.
38. Ryu, C.; Kim, S. J.; Kim, D.; Kaang, S.; Seo, G. The Effect of Surface Area of Silicas on Their Reinforcing Performance to Styrene-butadiene Rubber Compounds. *Elastomers Compos.* **2016**, 51, 128-137.
39. Surya, I.; Ismail, H.; Azura, A. R. The Comparison of Alkanol Amide and Silane Coupling Agent on the Properties of Silica-Filled Natural Rubber (SMR-L) Compounds. *Polym. Test.* **2014**, 40, 24-32.
40. Ravi Theja, M. S.; Kilari, N.; Vishvanathperumal, S.; Navaneethakrishnan, V. Modeling Tensile Modulus of Nanoclay-filled Ethylene–propylene–diene Monomer/styrene–butadiene Rubber Using Composite Theories. *J. Rubber Res.* **2021**, 24, 847-856.
41. Peng, H.; Liu, L.; Luo, Y.; Wang, X.; Jia, D. Effect of 3-Propionylthio-1-propyltrimethoxylsilane on Structure, Mechanical, and Dynamic Mechanical Properties of NR/Silica Composites. *Polym. Compos.* **2009**, 30, 955-961.
42. Vishvanathperumal, S.; Gopalakannan, S. Effects of the Nanoclay and Crosslinking Systems on the Mechanical Properties of Ethylene-propylene-diene Monomer/styrene Butadiene Rubber Blends Nanocomposite. *Silicon* **2019**, 11, 117-135.
43. Dileep, P.; Narayanankutty, S. K. Styrenated Phenol Modified Nanosilica for Improved Thermo-oxidative and Mechanical Properties of Natural Rubber. *Polym. Test.* **2020**, 82, 106302.
44. Zhang, X.; Cui, H.; Song, L.; Ren, H.; Wang, R.; He, A. Elastomer Nanocomposites with Superior Dynamic Mechanical Properties *via* Trans-1, 4-poly(butadiene-co-isoprene) Incorporation. *Compos. Sci. Technol.* **2018**, 158, 156-163.
45. Mostafa, A.; Kasem, A. A.; Bayoumi, M. R.; El-Sebaie, M. G. Effect of Carbon Black Loading on the Swelling and Compression Set Behavior of SBR and NBR Rubber Compounds. *Mater. Design* **2009**, 30, 1561-1568.
46. Aravinth, V.; Gurumoorthi, G.; Vishvanathperumal, S.; Navaneethakrishnan, V. Effect of Modified Nanographene Oxide on the Mechanical and Swelling Properties of Silicone Rubber Nanocomposites. *Polym. Korea* **2023**, 47, 288-302.
47. Govindan, K.; Ramabalan, S.; Vishvanathperumal, S.; Chockalingam, S., Influence of Halloysite Nanotubes on Mechanical and Swelling Properties of Silicone Rubber Compound. *J. Polym. Res.* **2023**, 30, 1-17.
48. Zhang, H.; Gao, Y.; Li, F.; Zhang, Z.; Liu, Y.; Zhao, G. Influence of Silane Coupling Agents on Vulcanised Natural Rubber: Dynamic Properties and Heat Buildup. *Plastics, Rubber and Compos* **2016**, 45, 9-15.